1-10-2000

Measurement of the Helicity of *W* Bosons in Top Quark Decays

T. Affolder
Ernest Orlando Lawrence Berkeley National Laboratory, Berkeley, California

Kenneth A. Bloom
University of Nebraska-Lincoln, kenbloom@unl.edu

Collider Detector at Fermilab Collaboration

Measurement of the Helicity of W Bosons in Top Quark Decays

T. Affolder,[21] H. Akimoto,[42] A. Akopian,[35] M. G. Albrow,[10] P. Amaral,[7] S. R. Amendolia,[31] D. Amidei,[24] J. Antos,[1] G. Apollinari,[35] T. Arisawa,[42] T. Asakawa,[40] W. Ashmanskas,[7] M. Atac,[10] P. Azzi-Bacchetta,[29] N. Bacchetta,[29] M. W. Bailey,[26] S. Bailey,[14] P. de Barbaro,[34] A. Barbaro-Galtieri,[21] V. E. Barnes,[33] B. A. Barnett,[17] M. Barone,[12] G. Bauer,[22] F. Bedeschi,[31] S. Belforte,[39] G. Bellettini,[31] J. Bellinger,[43] D. Benjamin,[9] J. Bensinger,[4] A. Beretvas,[10] J. P. Berge,[10] J. Berryhill,[7] S. Bertolucci,[12] B. Bevensee,[30] A. Bhatti,[35] C. Bigongiari,[31] M. Binkley,[10] D. Bisello,[29] R. E. Blair,[2] C. Blocker,[4] K. Bloom,[24] B. Blumenfeld,[17] B. S. Blusk,[34] A. Bocci,[31] A. Bodek,[34] W. Bokhari,[30] G. Bolla,[33] Y. Bonushkin,[5] D. Bortoletto,[33] J. Boudreau,[32] A. Brandl,[26] S. van den Brink,[17] C. Bromberg,[25] N. Bruner,[26] E. Buckley-Geer,[10] J. Budagov,[8] H. S. Budd,[34] K. Burkett,[14] G. Busetto,[29] A. Byon-Wagner,[10] K. L. Byrum,[2] M. Campbell,[24] A. Caner,[31] W. Carithers,[21] J. Carlson,[24] D. Carlsmith,[43] J. Cassada,[34] A. Castro,[29] D. Cauz,[39] A. Cerri,[31] P. S. Chang,[1] P. T. Chang,[1] J. Chapman,[24] C. Chen,[30] Y. C. Chen,[1] M.-T. Cheng,[1] M. Chertok,[37] G. Chiarelli,[31] I. Chirikov-Zorin,[8] G. Chlachidze,[8] F. Chlebana,[10] L. Christofek,[16] M. L. Chu,[1] S. Cihangir,[10] C. I. Ciobanu,[27] A. G. Clark,[13] M. Cobal,[31] E. Cocca,[31] A. Connolly,[21] J. Conway,[36] J. Cooper,[10] M. Cordelli,[12] D. Costanzo,[31] J. Cranshaw,[38] D. Cronin-Hennessy,[9] R. Cropp,[23] R. Culbertson,[7] D. Dagenhart,[41] F. DeJongh,[10] S. Dell'Agnello,[12] M. Dell'Orso,[31] R. Demina,[10] L. Demortier,[35] M. Deninno,[3] P. F. Derwent,[10] T. Devlin,[36] J. R. Dittmann,[10] S. Donati,[31] J. Done,[37] T. Dorigo,[14] N. Eddy,[16] K. Einsweiler,[21] J. E. Elias,[10] E. Engels, Jr.,[32] W. Erdmann,[10] D. Errede,[16] S. Errede,[16] Q. Fan,[34] R. G. Feild,[44] C. Ferretti,[31] I. Fiori,[3] B. Flaugher,[10] G. W. Foster,[10] M. Franklin,[14] J. Freeman,[10] J. Friedman,[22] Y. Fukui,[20] S. Gadomski,[23] S. Galeotti,[31] M. Gallinaro,[35] T. Gao,[30] M. Garcia-Sciveres,[21] A. F. Garfinkel,[33] P. Gatti,[29] C. Gay,[44] S. Geer,[10] D. W. Gerdes,[24] P. Giannetti,[31] P. Giromini,[12] V. Glagolev,[8] M. Gold,[26] J. Goldstein,[10] A. Gordon,[14] A. T. Goshaw,[9] Y. Gotra,[32] K. Goulianos,[35] H. Grassmann,[39] C. Green,[33] L. Groer,[36] C. Grosso-Pilcher,[7] M. Guenther,[33] G. Guillian,[24] J. Guimaraes da Costa,[24] R. S. Guo,[1] C. Haber,[21] E. Hafen,[22] S. R. Hahn,[10] C. Hall,[14] T. Handa,[15] R. Handler,[43] W. Hao,[38] F. Happacher,[12] K. Hara,[40] A. D. Hardman,[33] R. M. Harris,[10] F. Hartmann,[18] K. Hatakeyama,[35] J. Hauser,[5] J. Heinrich,[30] A. Heiss,[18] B. Hinrichsen,[23] K. D. Hoffman,[33] C. Holck,[30] R. Hollebeek,[30] L. Holloway,[16] R. Hughes,[27] J. Huston,[25] J. Huth,[14] H. Ikeda,[40] M. Incagli,[31] J. Incandela,[10] G. Introzzi,[31] J. Iwai,[42] Y. Iwata,[15] E. James,[24] H. Jensen,[10] M. Jones,[30] U. Joshi,[10] H. Kambara,[13] T. Kamon,[37] T. Kaneko,[40] K. Karr,[41] H. Kasha,[44] Y. Kato,[28] T. A. Keaffaber,[33] K. Kelley,[22] M. Kelly,[24] R. D. Kennedy,[10] R. Kephart,[10] D. Khazins,[9] T. Kikuchi,[40] M. Kirk,[4] B. J. Kim,[19] H. S. Kim,[23] S. H. Kim,[40] Y. K. Kim,[21] L. Kirsch,[4] S. Klimenko,[11] D. Knoblauch,[18] P. Koehn,[27] A. Köngeter,[18] K. Kondo,[42] J. Konigsberg,[11] K. Kordas,[23] A. Korytov,[11] E. Kovacs,[2] J. Kroll,[30] M. Kruse,[34] S. E. Kuhlmann,[2] K. Kurino,[15] T. Kuwabara,[40] A. T. Laasanen,[33] N. Lai,[7] S. Lami,[35] S. Lammel,[10] J. I. Lamoureux,[4] M. Lancaster,[21] G. Latino,[31] T. LeCompte,[2] A. M. Lee IV,[9] S. Leone,[31] J. D. Lewis,[10] M. Lindgren,[5] T. M. Liss,[16] J. B. Liu,[34] Y. C. Liu,[1] N. Lockyer,[30] M. Loreti,[29] D. Lucchesi,[29] P. Lukens,[10] S. Lusin,[43] J. Lys,[21] R. Madrak,[14] K. Maeshima,[10] P. Maksimovic,[14] L. Malferrari,[3] M. Mangano,[31] M. Mariotti,[29] G. Martignon,[29] A. Martin,[44] J. A. J. Matthews,[26] P. Mazzanti,[3] K. S. McFarland,[34] P. McIntyre,[37] E. McKigney,[30] M. Menguzzato,[29] A. Menzione,[31] E. Meschi,[31] C. Mesropian,[35] C. Miao,[24] T. Miao,[10] R. Miller,[25] J. S. Miller,[24] H. Minato,[40] S. Miscetti,[12] M. Mishina,[20] N. Moggi,[31] E. Moore,[26] R. Moore,[24] Y. Morita,[20] A. Mukherjee,[10] T. Muller,[18] A. Munar,[31] P. Murat,[31] S. Murgia,[25] M. Musy,[39] J. Nachtman,[5] S. Nahn,[44] H. Nakada,[40] T. Nakaya,[7] I. Nakano,[15] C. Nelson,[10] D. Neuberger,[18] C. Newman-Holmes,[10] C.-Y. P. Ngan,[22] P. Nicolaidi,[39] H. Niu,[4] L. Nodulman,[2] A. Nomerotski,[11] S. H. Oh,[9] T. Ohmoto,[15] T. Ohsugi,[15] R. Oishi,[40] T. Okusawa,[28] J. Olsen,[43] C. Pagliarone,[31] F. Palmonari,[31] R. Paoletti,[31] V. Papadimitriou,[38] S. P. Pappas,[44] A. Parri,[12] D. Partos,[4] J. Patrick,[10] G. Pauletta,[39] M. Paulini,[21] A. Perazzo,[31] L. Pescara,[29] T. J. Phillips,[9] G. Piacentino,[31] K. T. Pitts,[10] R. Plunkett,[10] A. Pompos,[33] L. Pondrom,[43] G. Pope,[32] F. Prokoshin,[8] J. Proudfoot,[2] F. Ptohos,[12] G. Punzi,[31] K. Ragan,[23] D. Reher,[21] A. Ribon,[29] F. Rimondi,[3] L. Ristori,[31] W. J. Robertson,[9] A. Robinson,[23] T. Rodrigo,[6] S. Rolli,[41] L. Rosenson,[22] R. Roser,[10] R. Rossin,[29] W. K. Sakumoto,[34] D. Saltzberg,[5] A. Sansoni,[12] L. Santi,[39] H. Sato,[40] P. Savard,[23] P. Schlabach,[10] E. E. Schmidt,[10] M. P. Schmidt,[44] M. Schmitt,[14] L. Scodellaro,[29] A. Scott,[5] A. Scribano,[31] S. Segler,[10] S. Seidel,[26] Y. Seiya,[40] A. Semenov,[8] F. Semeria,[3] T. Shah,[22] M. D. Shapiro,[21] P. F. Shepard,[32] T. Shibayama,[40] M. Shimojima,[40] M. Shochet,[7] J. Siegrist,[21] G. Signorelli,[31] A. Sill,[38] P. Sinervo,[23] P. Singh,[16] A. J. Slaughter,[44] K. Sliwa,[41] C. Smith,[17] F. D. Snider,[10] A. Solodsky,[35] J. Spalding,[10] T. Speer,[13] P. Sphicas,[22] F. Spinella,[31] M. Spiropulu,[14] L. Spiegel,[10] L. Stanco,[29] J. Steele,[43] A. Stefanini,[31] J. Strologas,[16] F. Strumia,[13] D. Stuart,[10] K. Sumorok,[22] T. Suzuki,[40] R. Takashima,[15] K. Takikawa,[40] M. Tanaka,[40] T. Takano,[28] B. Tannenbaum,[5] W. Taylor,[23] M. Tecchio,[24] P. K. Teng,[1] K. Terashi,[40] S. Tether,[22] D. Theriot,[10] R. Thurman-Keup,[2]

 0031-9007/00/84(2)/216(6)$15.00

P. Tipton,[34] S. Tkaczyk,[10] K. Tollefson,[34] A. Tollestrup,[10] H. Toyoda,[28] W. Trischuk,[23] J. F. de Troconiz,[14] S. Truitt,[24] J. Tseng,[22] N. Turini,[31] F. Ukegawa,[40] J. Valls,[36] S. Vejcik III,[10] G. Velev,[31] R. Vidal,[10] R. Vilar,[6] I. Vologouev,[21] D. Vucinic,[22] R. G. Wagner,[2] R. L. Wagner,[10] J. Wahl,[7] N. B. Wallace,[36] A. M. Walsh,[36] C. Wang,[9] C. H. Wang,[1] M. J. Wang,[1] T. Watanabe,[40] T. Watts,[36] R. Webb,[37] H. Wenzel,[18] W. C. Wester III,[10] A. B. Wicklund,[2] E. Wicklund,[10] H. H. Williams,[30] P. Wilson,[10] B. L. Winer,[27] D. Winn,[24] S. Wolbers,[10] D. Wolinski,[24] J. Wolinski,[25] S. Worm,[26] X. Wu,[13] J. Wyss,[31] A. Yagil,[10] W. Yao,[21] G. P. Yeh,[10] P. Yeh,[1] J. Yoh,[10] C. Yosef,[25] T. Yoshida,[28] I. Yu,[19] S. Yu,[30] A. Zanetti,[39] F. Zetti,[21] and S. Zucchelli[3]

(CDF Collaboration)

[1]*Institute of Physics, Academia Sinica, Taipei, Taiwan 11529, Republic of China*
[2]*Argonne National Laboratory, Argonne, Illinois 60439*
[3]*Istituto Nazionale di Fisica Nucleare, University of Bologna, I-40127 Bologna, Italy*
[4]*Brandeis University, Waltham, Massachusetts 02254*
[5]*University of California at Los Angeles, Los Angeles, California 90024*
[6]*Instituto de Fisica de Cantabria, University of Cantabria, 39005 Santander, Spain*
[7]*Enrico Fermi Institute, University of Chicago, Chicago, Illinois 60637*
[8]*Joint Institute for Nuclear Research, RU-141980 Dubna, Russia*
[9]*Duke University, Durham, North Carolina 27708*
[10]*Fermi National Accelerator Laboratory, Batavia, Illinois 60510*
[11]*University of Florida, Gainesville, Florida 32611*
[12]*Laboratori Nazionali di Frascati, Istituto Nazionale di Fisica Nucleare, I-00044 Frascati, Italy*
[13]*University of Geneva, CH-1211 Geneva 4, Switzerland*
[14]*Harvard University, Cambridge, Massachusetts 02138*
[15]*Hiroshima University, Higashi-Hiroshima 724, Japan*
[16]*University of Illinois, Urbana, Illinois 61801*
[17]*The Johns Hopkins University, Baltimore, Maryland 21218*
[18]*Institut für Experimentelle Kernphysik, Universität Karlsruhe, 76128 Karlsruhe, Germany*
[19]*Korean Hadron Collider Laboratory: Kyungpook National University, Taegu 702-701, Korea and Seoul National University, Seoul 151-742, Korea and SungKyunKwan University, Suwon 440-746, Korea*
[20]*High Energy Accelerator Research Organization (KEK), Tsukuba, Ibaraki 305, Japan*
[21]*Ernest Orlando Lawrence Berkeley National Laboratory, Berkeley, California 94720*
[22]*Massachusetts Institute of Technology, Cambridge, Massachusetts 02139*
[23]*Institute of Particle Physics: McGill University, Montreal, Canada H3A 2T8 and University of Toronto, Toronto, Canada M5S 1A7*
[24]*University of Michigan, Ann Arbor, Michigan 48109*
[25]*Michigan State University, East Lansing, Michigan 48824*
[26]*University of New Mexico, Albuquerque, New Mexico 87131*
[27]*The Ohio State University, Columbus, Ohio 43210*
[28]*Osaka City University, Osaka 588, Japan*
[29]*Universita di Padova, Istituto Nazionale di Fisica Nucleare, Sezione di Padova, I-35131 Padova, Italy*
[30]*University of Pennsylvania, Philadelphia, Pennsylvania 19104*
[31]*Istituto Nazionale di Fisica Nucleare, University and Scuola Normale Superiore of Pisa, I-56100 Pisa, Italy*
[32]*University of Pittsburgh, Pittsburgh, Pennsylvania 15260*
[33]*Purdue University, West Lafayette, Indiana 47907*
[34]*University of Rochester, Rochester, New York 14627*
[35]*Rockefeller University, New York, New York 10021*
[36]*Rutgers University, Piscataway, New Jersey 08855*
[37]*Texas A&M University, College Station, Texas 77843*
[38]*Texas Tech University, Lubbock, Texas 79409*
[39]*Istituto Nazionale di Fisica Nucleare, University of Trieste, Udine, Italy*
[40]*University of Tsukuba, Tsukuba, Ibaraki 305, Japan*
[41]*Tufts University, Medford, Massachusetts 02155*
[42]*Waseda University, Tokyo 169, Japan*
[43]*University of Wisconsin, Madison, Wisconsin 53706*
[44]*Yale University, New Haven, Connecticut 06520*

(Received 26 August 1999)

We use the transverse momentum spectrum of leptons in the decay chain $t \to bW$ with $W \to l\nu$ to measure the helicity of the W bosons in the top quark rest frame. Our measurement uses a $t\bar{t}$ sample isolated in 106 ± 4 pb^{-1} of data collected in $p\bar{p}$ collisions at $\sqrt{s} = 1.8$ TeV with the CDF detector at

the Fermilab Tevatron. Assuming a standard V-A weak decay, we find that the fraction of W's with zero helicity in the top rest frame is $\mathcal{F}_0 = 0.91 \pm 0.37(\text{stat}) \pm 0.13(\text{syst})$, consistent with the standard model prediction of $\mathcal{F}_0 = 0.70$ for a top mass of 175 GeV/c^2.

PACS numbers: 14.65.Ha, 12.15.Ji, 12.60.Cn, 13.88.+e

The weak decays of the top quark should be described by the universal V-A charged-current interactions of the standard model. The theory makes a specific prediction for the polarization state of the W bosons, which can be measured using the lepton momentum spectrum in the decay chain $t \to bW$ with $W \to l\nu$. Observation of the predicted lepton momentum spectrum can verify that the signal observed at the Tevatron is the standard model top quark.

In top decays with a pure V-A coupling the amplitude for positive helicity W^+ bosons is suppressed by the chiral factors of order m_b^2/M_W^2, and the W helicity is a superposition of just the zero and negative helicity states [1]. At tree level in the standard model, the relative fraction $\mathcal{F}_0$ of the longitudinal (or zero helicity) W's in the top rest frame is predicted to be [2]

$$\mathcal{F}_0 = \frac{m_t^2/2M_W^2}{1 + m_t^2/2M_W^2} = (70.1 \pm 1.6)\% . \qquad (1)$$

This expression is valid for $m_t > M_W$ and is evaluated at the measured value of $m_t = 174.3 \pm 5.1$ GeV/c^2 [3]. In the standard model, the dominance of the zero helicity state can be interpreted in terms of the large top Yukawa coupling to the longitudinal mode of the W. However, this result does not depend on the symmetry breaking mechanism of the standard model and is valid as long as the interaction is $V \pm A$, the particles have their assumed spins, and Lorentz invariance holds.

Nonstandard spins in the Tevatron top signal could arise from a supersymmetric scalar top component, as suggested in Ref. [4]. Alternatively, effective Lagrangian treatments can also be used to relate the value of $\mathcal{F}_0$ to the strength of nonstandard decay couplings [2,5]. Indirect limits on such couplings have been derived from precision b quark measurements [6,7]. The strictest of these uses the measured rate of $b \to s\gamma$ to limit the size of a $V + A$ contribution to top decay to less than a few percent [7,8]. We address the matter of a direct test for a $V + A$ contribution in top decay separately at the end of this paper.

We will use $\mathcal{F}_0$ to parametrize the agreement between the predicted and measured lepton momentum spectrum in top decay. Our measurement utilizes $t\bar{t}$ decays where one or both of the W bosons from top decay leptonically. The V-A coupling at the lepton vertex induces a strong correlation between the W helicity and lepton momentum which survives into the lab frame. Charged leptons from negative helicity W are softer than the charged leptons from longitudinal W bosons. In Figure 1 we show the expected lepton transverse momentum (P_T) in the laboratory frame [9] for the three W helicities. These spectra are generated from a custom version of the HERWIG Monte Carlo program with adjustable W helicity amplitudes [10], followed by a complete simulation of the detector effects. The lepton P_T clearly provides good discrimination between the different W helicity states. The threshold at 20 GeV/c is a result of our event selection and will be discussed below.

To measure $\mathcal{F}_0$ we model the lepton P_T in $t \to bl\nu$ according to the standard model as a superposition of the W boson negative and zero helicity distributions in Fig. 1 and then use a maximum likelihood method to find the relative ratio which best fits the data. Our measurement uses a $t\bar{t}$ sample isolated in 106 ± 4 pb^{-1} of data collected in $p\bar{p}$ collisions at $\sqrt{s} = 1.8$ TeV with the CDF detector at the Fermilab Tevatron. The detector is described in [11].

Decays of $t\bar{t}$ pairs with a single lepton, called lepton + jet events, are characterized by a single isolated high P_T electron or muon, missing transverse energy ($\not\!\!E_T$) from the neutrino in the $W \to l\nu$ decay, and four jets, two from the hadronically decaying W boson and two from the b quarks. Our lepton + jet sample is selected by requiring a single electron or muon with $P_T > 20$ GeV/c which is isolated from jet activity, $\not\!\!E_T > 20$ GeV, and at least three jets with measured $E_T > 15$ GeV.

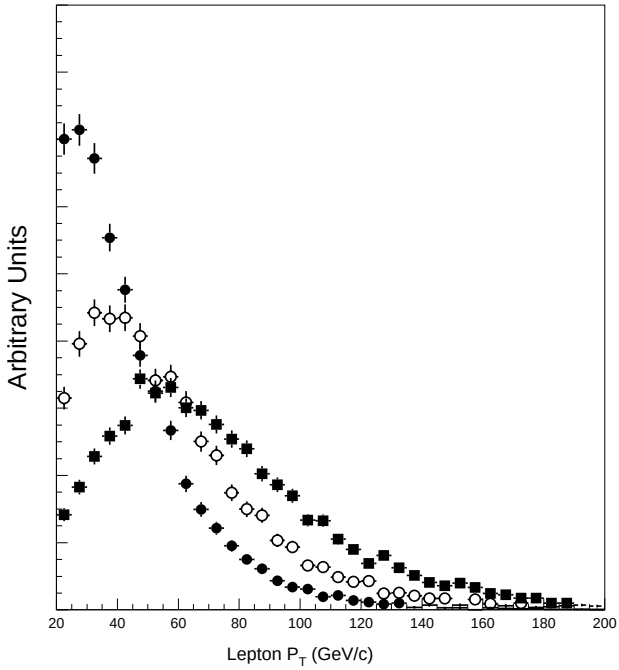

FIG. 1. Lepton P_T distributions for the three W helicities. The solid circles are from negative helicity W^+ and positive helicity W^-, the open circles are from longitudinal W^+ and W^-, and the closed squares are from positive helicity W^+ and negative helicity W^-. All three distributions are normalized to the same area.

We divide the lepton + jet events into subsamples based on three selections with different top purities. In the silicon vertex tracker (SVX) tag sample, we require at least one of the jets in the event to be identified as a b jet candidate by reconstructing a secondary vertex from the b quark decay using the silicon vertex tracker. The SVX tagging algorithm is described in [12]. In the soft lepton tag (SLT) sample, we require that one or more jets be identified as a b jet candidate by identifying an additional lepton in the event, which is presumed to come from a semileptonic b decay (see [12]). We also require a fourth jet in the event which has $E_T > 8$ GeV and $|\eta| < 2.4$. Events that satisfy the requirements of both the SVX and SLT samples are considered to be SVX events and are removed from the SLT tag sample. In the no-tag sample, we require a fourth jet in the event with $E_T > 15$ GeV and $|\eta| < 2.0$. The backgrounds in the SVX sample are described in [13], while those in the no-tag and SLT tag sample are given in [14].

Events where both W's from top decay into leptons, called dilepton events, are characterized by an electron or muon plus $\not\!\!E_T$ from each of the two $W \rightarrow l\nu$ decays, and two jets from the b quarks. The two leptons must be oppositely charged. The selection requirements and backgrounds we use for the dilepton sample are described in [15]. We make the additional requirement that the two leptons not be of the same flavor. This cut removes a background from Drell-Yan events with large $\not\!\!E_T$ for which we have no good lepton P_T model. It removes two of the nine events in the standard CDF dilepton analysis (see Ref. [15]) but reduces the background from 2.4 ± 0.5 to 0.76 ± 0.21 events, for an overall gain in purity.

The largest source of background in the lepton + jet sample consists of W bosons produced with associated jets, called W + jets events. We model these, as well as other smaller contributions, using VECBOS [16], a Monte Carlo program that has been shown to be a good representation of these processes [17]. A smaller, but still significant lepton + jet background, $(23 \pm 5)\%$ averaged across the three lepton + jet subsamples, comes from non-W events, i.e., fake leptons and heavy quark production. We use lepton + jet data events, in which the lepton is embedded in jet activity and fails our lepton isolation requirement for the top sample, to model these backgrounds.

The background to the dilepton sample comes from $Z \rightarrow \tau\tau, WW, WZ$, and ZZ production, and fake lepton events where a jet passes our lepton identification cuts. We model these backgrounds using a combination of the PYTHIA and ISAJET Monte Carlo generators [18,19] and CDF data [15].

We summarize in Table I the number of events and the predicted amount of background in each data sample. Note that the dilepton sample contributes two entries for each event.

We use an unbinned log-likelihood function to estimate the fraction of top quarks that decay to longitudinal W bosons. Let $\mathcal{P}^S(P_T; \mathcal{F}_0, m_t)$ be the probability density to obtain a lepton with transverse momentum P_T from a top quark of mass m_t and longitudinal fraction $\mathcal{F}_0$. To obtain $\mathcal{P}^S$ we generate two samples of $t\bar{t}$ events at mass m_t, using the HERWIG Monte Carlo generator in concert with a full detector simulation. In one sample top decays only to negative helicity W bosons and in the other top decays only to longitudinal W bosons. We then parametrize the lepton P_T spectrum of each sample as the product of an exponential and a polynomial. We add the resulting functions together, using the factors $1 - \mathcal{F}_0$ and $\mathcal{F}_0$ as weights for the respective components. This yields the probability density $\mathcal{P}^S$ as a smooth function of $\mathcal{F}_0$ and a discrete function of m_t. The probability density $\mathcal{P}^B(P_T)$ of finding a lepton with transverse momentum P_T in the background to our top signal is obtained via a similar parametrization of background model lepton P_T distributions. Both $\mathcal{P}^S$ and $\mathcal{P}^B$ are normalized to a probability of 1 above the lepton P_T threshold of 20 GeV/c.

The negative log-likelihood is the sum of two terms:

$$-\log\mathcal{L} = -\log\mathcal{L}_{\text{shape}} - \log\mathcal{L}_{\text{backgr}}, \qquad (2)$$

where $\mathcal{L}_{\text{shape}}(m_t, x_b, \mathcal{F}_0)$ represents the joint probability density for a sample of N leptons with transverse momenta P_{Ti} to be drawn from a population of top candidate events with mass m_t, background fraction x_b, and longitudinal W fraction $\mathcal{F}_0$:

$$\mathcal{L}_{\text{shape}} = \prod_{i=1}^{N} [(1 - x_b)\mathcal{P}^S(P_{Ti}; \mathcal{F}_0, m_t) + x_b\mathcal{P}^B(P_{Ti})]. \qquad (3)$$

We compute the log-likelihood for each of our analysis subsamples separately and then add them together and minimize them simultaneously. The $\mathcal{L}_{\text{backgr}}$ term in Eq. (2) is included to allow us to constrain the background fraction x_b to the expected values as shown in Table I (see [13–15]). The shape of this background constraint varies from sample to sample and depends upon how the background in the sample was calculated.

Note that in constructing $\mathcal{P}^S$, we normalized the probability densities for leptons from both negative helicity and longitudinal W bosons to unit area above the 20 GeV/c lepton P_T acceptance threshold. This choice of normalizations guarantees that Eq. (3) is linear in $\mathcal{F}_0$. However, the stiffer leptons from longitudinal W decays are 30% more likely to pass the lepton P_T acceptance cut than leptons from negative helicity W decays, so our fit tends to overestimate $\mathcal{F}_0$. We apply a *post facto* correction to $\mathcal{F}_0$ to account for this bias. The correction is a simple algebraic function of the measured $\mathcal{F}_0$; its magnitude varies between -0.08, when $\mathcal{F}_0$ is near 0.5, and 0.0, when $\mathcal{F}_0$ is near 0 or 1.

We minimize the log-likelihood with respect to $\mathcal{F}_0$ at a top mass of 175 GeV/c^2 and obtain $\mathcal{F}_0 = 0.91 \pm 0.37$, after subtracting 0.02 from the result of the minimization to account for the acceptance bias. The statistical uncertainty corresponds to a half-unit change in the

TABLE I. Result of measurements for $\mathcal{F}_0$ and description of sample content. The fifth column lists the measurement after a correction for an acceptance bias is applied. Note that our acceptance correction is undefined for unphysical values of $\mathcal{F}_0$. Each dilepton event enters twice in the last row.

Sample	Events	Background	$\mathcal{F}_0$	Corrected $\mathcal{F}_0$
SVX tagged	34	9.2 ± 1.2	$0.92^{+0.41}_{-0.41}$	$0.90^{+0.46}_{-0.46}$
SLT tagged	14	6.0 ± 1.2	$-0.07^{+0.91}_{-0.27}$	$-0.07^{+0.87}_{-0.27}$
No tag	46	25.9 ± 6.5	$1.15^{+0.98}_{-0.70}$	$1.15^{+0.98}_{-0.77}$
Dilepton	7	0.76 ± 0.21	$0.60^{+0.57}_{-0.47}$	$0.56^{+0.57}_{-0.45}$
Total leptons	108	42.6 ± 6.7	$0.93^{+0.32}_{-0.32}$	$0.91^{+0.37}_{-0.37}$

negative log-likelihood with respect to the minimum. In Fig. 2 we compare $\mathcal{L}_{\text{shape}}$ to the lepton + jet and dilepton data distributions. We summarize the measurement of $\mathcal{F}_0$ in Table I. Included in this table are the results of measurements performed separately in each subsample.

The systematic uncertainties associated with this measurement of $\mathcal{F}_0$ are listed in Table II. The largest possible error is due to the uncertainty on the top quark mass, because the lepton P_T spectrum depends upon the mass of the top. The magnitude of the effect is estimated by repeating the analysis on Monte Carlo samples where we vary the top mass. For $\delta M_t = 5.1\ \text{GeV}/c^2$, $\delta\mathcal{F}_0 = 0.07$ [3].

Another significant systematic uncertainty is due to background normalization. The lepton P_T spectrum for non-W processes peaks at low P_T, mimicking the shape from negative helicity W bosons. The effect on our measurement is estimated by varying the amount of non-W contribution in our background shapes within the envelope of normalization errors. We must also account for a 20% uncertainty in the tagging efficiency of the SVX algorithm; this causes a ± 0.05 uncertainty in the measurement of $\mathcal{F}_0$. Other sources of uncertainty include the limits on the generation of Monte Carlo statistics, the acceptance bias introduced by the selection cut on the transverse momentum of the lepton, the shape of the non-W background, the modeling of initial and final state gluon radiation in our Monte Carlo samples, and the parton distribution functions. Our final result is $\mathcal{F}_0 = 0.91 \pm 0.37(\text{stat}) \pm 0.13(\text{syst})$.

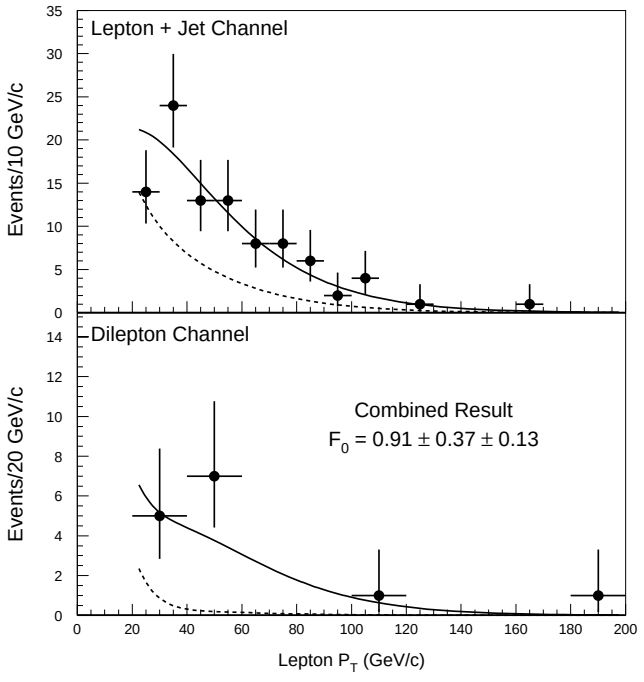

FIG. 2. Lepton P_T distributions for the lepton + jet and dilepton subsamples. The lepton + jet subsamples are added together to simplify presentation. The data (points) are compared with the result of the combined fit (solid line) and with the background component of the fit (dashed line).

Finally, we return to the question of a $V + A$ component in top decay. Although the indirect limit from $b \to s\gamma$ is already severe, we can still use our technique to search directly for a $V + A$ component in the lepton P_T spectrum. As shown in Fig. 1, the momentum of leptons from positive helicity W^+ are harder than those with negative or longitudinal helicity. We have accordingly generalized our $\mathcal{L}_{\text{shape}}$ to include the positive helicity fraction $\mathcal{F}_+$. When we fit the lepton P_T spectrum for all three components simultaneously, we find no statistical sensitivity within our data set. As an alternative, we hold $\mathcal{F}_0$ constant at its standard model value and fit for the superposition of positive and negative helicity W's, yielding a positive helicity fraction $\mathcal{F}_+ = 0.11 \pm 0.15$.

In summary, we have compared the lepton P_T spectrum in semileptonic decays $t \to bW \to bl\nu$ to the predictions of the standard electroweak model for top quark

TABLE II. List of systematic uncertainties in the measurement of the helicity of W bosons in top decays.

Source	Uncertainty in $\mathcal{F}_0$
Top mass uncertainty	0.07
Non-W background normalization	0.06
b-tag efficiency	0.05
Monte Carlo statistics	0.05
Acceptance uncertainties	0.02
Non-W background shape	0.04
Gluon radiation	0.03
Parton distribution functions	0.02
Total uncertainty	0.13

decay. Assuming a pure V-A coupling, we measure the fraction of longitudinal W bosons in top quark decays to be $0.91 \pm 0.37(\text{stat}) \pm 0.13(\text{syst})$. This measurement is consistent with the prediction of 0.70 for top quarks of mass 174.3 GeV$/c^2$.

We thank the Fermilab staff and the technical staffs of the participating institutions for their vital contributions. This work is supported by the U.S. Department of Energy and the National Science Foundation, the Natural Sciences and Engineering Research Council of Canada, the Istituto Nazionale di Fisica Nucleare of Italy, the Ministry of Education, Science and Culture of Japan, the National Science Council of the Republic of China, and the A. P. Sloan Foundation.

[1] Reference to the decay $t \to bW^+ \to bl^+\nu$ implicitly includes the charge-parity conjugate decay $\bar{t} \to \bar{b}W^- \to \bar{b}l^-\bar{\nu}$, in which the W^- is in a superposition of the positive helicity and longitudinal states.

[2] R. Peccei and X. Zhang, Nucl. Phys. **B337**, 269 (1990); G. L. Kane, G. A. Ladinsky, and C.-P. Yuan, Phys. Rev. D **45**, 124 (1992); R. H. Dalitz and G. R. Goldstein, Phys. Rev. D **45**, 1531 (1992); M. Jezabek and J. H. Kuhn, Phys. Lett. B **329**, 317 (1994); C. A. Nelson, B. T. Kress, M. Lopes, and T. P. McCauley, Phys. Rev. D **56**, 5928 (1997).

[3] L. Demortier, R. Hall, R. Hughes, B. Klima, R. Roser, and M. Strovink, Fermilab Report No. FERMILAB-TM-2084, 1999.

[4] C.-L. Chou and M. E. Peskin, hep-ph/9909536.

[5] For example, a measurement of $\mathcal{F}_0$ with an accuracy of 5% is sensitive to a chiral $f_M + f_E$-type coupling with 20% of the weak strength. S. Willenbrock, in *Particle Theory and Phenomenology: Proceedings*, edited by K. E. Lassila, J. Qiu, A. Sommerer, G. Valencia, K. Whisnat, and B. L. Young (World Scientific, Singapore, 1996), pp. 8–15.

[6] S. Dawson and G. Valencia, Phys. Rev. D **53**, 1721 (1996).

[7] M. Hosch, K. Whisnant, and Bing-Lin Young, Phys. Rev. D **55**, 3137 (1997).

[8] M. S. Alam *et al.*, Phys. Rev. Lett. **74**, 2885 (1995); K. Fujikawa and A. Yamada, Phys. Rev. D **49**, 5890 (1994); J. L. Hewett and T. G. Rizzo, Phys. Rev. D **49**, 319 (1994).

[9] In the CDF coordinate system, θ and ϕ are the polar and azimuthal angles, respectively, with respect to the proton beam direction (z axis). The pseudorapidity η is defined as $-\ln\tan(\frac{\theta}{2})$. The transverse momentum of a particle is $P_T = P\sin\theta$. The analogous quantity using calorimeter energies, defined as $E_T = E\sin\theta$, is called transverse energy. The missing transverse energy, $\not\!\!E_T$, is defined as $-\sum E_T^i \hat{n}_i$, where $\hat{n}_i$ are the transverse components of the unit vectors pointing from the interaction point to the energy deposition in the calorimeter (i runs over the calorimeter cells).

[10] G. Marchesini and B. R. Webber, Nucl. Phys. **B310**, 461 (1988); G. Marchesini *et al.*, Comput. Phys. Commun. **67**, 465 (1992).

[11] F. Abe *et al.*, Nucl. Instrum. Methods Phys. Res., Sect. A **271**, 387 (1988); D. Amidei *et al.*, *ibid.* **350**, 73 (1994); P. Azzi *et al.*, *ibid.* **360**, 137 (1995).

[12] F. Abe *et al.*, Phys. Rev. Lett. **74**, 2626 (1995).

[13] F. Abe *et al.*, Phys. Rev. Lett. **80**, 2773 (1998).

[14] F. Abe *et al.*, Phys. Rev. Lett. **80**, 2767 (1998). The CDF top mass analysis requires events to pass an additional "goodness of fit" cut based upon the kinematic fitter which is used to reconstruct the top mass. We use the efficiency of this cut to extrapolate the mass analysis backgrounds to the backgrounds required for this analysis, where no goodness of fit cut is applied.

[15] F. Abe *et al.*, Phys. Rev. Lett. **80**, 2779 (1998).

[16] F. A. Berends, W. T. Giele, H. Kuijf, and B. Tausk, Nucl. Phys. **B357**, 32 (1991).

[17] F. Abe *et al.*, Phys. Rev. Lett. **73**, 2296 (1994); F. Abe *et al.*, Fermilab Report No. Fermilab-Pub-98/327-E.

[18] T. Sjöstrand, Comput. Phys. Commun. **82**, 74 (1994). We use PYTHIA version 5.7.

[19] F. Paige and S. Protopopescu, BNL Report No. 38034, 1986 (unpublished). We use ISAJET version 7.06.